Spatial Augmented Reality for Heavy Machinery using Laser Projections

Thomas Kernbauer* Maximilian Tschulik† Philipp Fleck‡ and Clemens Arth§
Institute of Computer Graphics and Vision
Graz University of Technology

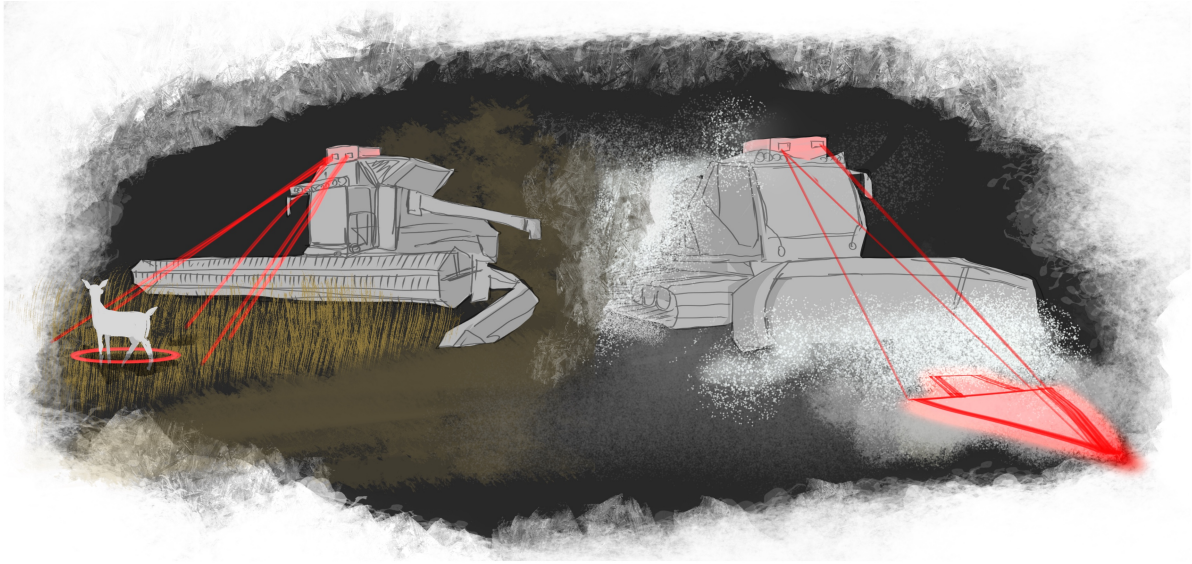

Figure 1: Concept drawing of potential applications with the proposed laser projection-based AR setup. On the left, a harvester and some animal are shown, which is highlighted to inform the operator. On the right, a snow groomer is shown with the laser projector indicating the proposed direction of movement.

ABSTRACT

Operating heavy machinery is challenging and can pose safety hazards for the operator and bystanders. Although commonly used augmented reality (AR) devices, such as head-mounted or head-up displays, can provide occupational support to operators, they can also cause problems. Particularly in off-highway scenarios, i.e., when driving machines in bumpy environments, the usefulness of current AR devices and the willingness of operators to wear them are limited. Therefore, we explore how laser-projection-based AR can help the operator facilitate their tasks and enhance safety. For this, we present a compact hardware unit and introduce a flexible and declarative software system. Furthermore, we examine the calibration process to leverage a camera projector setup and outline a process for creating images suitable for display by a laser projector from a set of line segments. Finally, we showcase its ability to provide efficient instructions to operators and bystanders and propose concrete applications for our setup.

Index Terms: Human-centered computing—Visualization—Visualization design and evaluation methods

1 INTRODUCTION

Maneuvering and controlling heavy machinery, such as excavators, harvesters, or snow groomers, in uneven terrain and under various weather and lightning conditions is undoubtedly a complex task. Operators require a wide range of skills, including an immersive understanding of the environment and quick decision-making. If well integrated, sensory information can help the operator in his workflow and enhance these skills. While the benefits of common AR devices, such as head-up displays (HUDs) or head-mounted displays (HMDs), in certain domains are undeniable, it is crucial to examine their applicability in contexts of heavy machinery.

HMDs, widely used for virtual reality (VR) and AR applications, can cause motion sickness [14], even if used in a static setting. This problem is exacerbated because the cabins in heavy machinery exhibit substantial movement and heavy vibrations. Furthermore, blocking the operator's field of view (FOV) may hinder the observation of vital information, which can potentially lead to oversights and accidents. Furthermore, prolonged use of HMDs can cause ergonomic discomfort and strain the operator [6].

Other AR setups, such as HUDs use projections on the windscreen and, therefore, require tracking the viewer's position to render overlays on the environment. However, these displays are found to increase the mental workload required [19] when utilized in the context of vehicle operation. In addition, a recent study [25] notes the lack of available HUDs with sufficient optical aspect ratios for heavy machinery operation and emphasizes the need for more mechanical and optical development.

In this work, we propose projection-based AR for off-highway vehicles (see Fig. 1). With our setup, we project information directly into the environment, visible to bystanders and operators. This enables additional use cases, such as collaboration between the operator and co-workers outside the vehicle or the display of warnings for everyone around. Moreover, our solution does not require any tracking and is able to project primitives on a large portion of the operator's FOV. We present an independent hardware unit containing a laser projector, a camera, and a local controller as a projection-based AR development platform for heavy machinery.

*e-mail: thomas.kernbauer@icg.tugraz.at
†e-mail: maximilian.tschulik@student.tugraz.at
‡e-mail: philipp.fleck@icg.tugraz.at
§e-mail: arth@icg.tugraz.at

Furthermore, we introduce a software system for this unit with a flexible network-based interface capable of creating and optimizing images for laser projectors from a set of geometric primitives. We look into the calibration of the camera-projector setup using existing calibration methods and implement a way to reconstruct geometric information about the projection surface. This allows us to project the primitives with a viewpoint correction, thus creating seemingly undistorted views for the operator. Additionally, we implement the projection of points in the world onto the projector image, enabling us to project points or lines to arbitrary positions in the 3D world using the laser projector.

The rest of this document is organized as follows. Sect. 2 examines prior research, while Sect. 3 provides information on the calibration and correction of a laser-camera projection system. In Sect. 4, we offer a comprehensive account of our prototype and thoroughly explain the steps involved in our laser projection pipeline, which encompasses various crucial yet difficult tasks. The results of our experiments are presented in Sect. 5, followed by a discussion in Sect. 6. Concluding remarks can be found in Sect. 7.

2 Related Work

The concept of using projectors to augment reality on real-world surfaces, known as spatial augmented reality (SAR), dates back to as early as 1999 [21]. Furthermore, AR has found substantial application in the field of heavy machinery operation. In the following, we provide a summary of previous research in the SAR domain, along with an overview of approaches w.r.t. to AR and its utilization in heavy machinery operations. Furthermore, we concisely summarize the camera-laser calibration approaches.

2.1 Spatial Augmented Reality

Raskar *et al*. [21] introduced SAR as a camera projector setup to extract information about the projection surface together with a method to render virtual 3D objects for a head-tracked user. They list the independence of a head-mounted display as a key benefit of SAR compared to other AR setups. Subsequent research on SAR, *e.g.,* Shader Lamps [22], focuses on creating realistic projections in static scenes by using projectors to change the shading of real-world objects, simulating different materials and textures. Their setup requires both the projector and the model to be static. Using a combination of additional sensors, such as a camera or a tilt sensor, iLamps [20] allows usage in dynamic scenes, as the projector adapts to its environment automatically.

Approaches that employ laser projectors for SAR are less common. Schwerdtfeger *et al*. [24] explores the use of laser projectors for industrial AR applications. They experimented with two different sets of lights, *i.e.,* a mobile projector mounted on a head and a semi-stationary projector mounted on a tripod. Glossop and Wang [10] use a laser projection-based AR setup for computer-assisted surgeries that project markers directly onto a patient's skull. This application requires high accuracy, which is achieved using a manually calibrated stationary projector positioned approximately orthogonal to the projection surface. Another example of a stationary laser projection-based AR setup can be found in [29], where the authors use a tracked input device to draw a trajectory visualized by a laser projector to program an industrial robot.

2.2 Augmented Reality in Heavy Machinery

AR is used in a multitude of applications to support operators in heavy machinery vehicles [25]. The area of application includes in-cabin support, *e.g.,* applying diminished reality to remove obstructions in the field-of-view (FOV) [2], as well as enhancing the experience of remote controlled vehicles (*i.e.,* teleoperated) [7]. According to [25], the types of heavy machinery featured in AR-supported applications include cranes [8], tractors [16], forklifts [23], and excavators [28].

In terms of devices and visualization technologies used, the majority of applications utilize video-based AR, *i.e.,* information on video streams, or see-through devices, such as HMDs or HUDs. However, as Sitompul and Wallmyr [25] note, the FOV of HUDs is too restricted to be applicable in heavy machinery cabins. In addition to in-cabin support, HMDs are commonly used in the context of remote vehicle operation [11, 23].

2.3 Camera-Laser Calibration

Tsai [27] introduced a popular camera calibration technique using a single image of a coplanar calibration object to estimate the camera's optical parameters and relative position. Later, Zhang [30] proposed a more robust method using multiple images of a planar calibration target, which can be easily created using a regular printer. This calibration method became one of the most commonly used techniques to calibrate cameras due to its ease of use and robustness.

Moreno and Taubin [17] describe the calibration of a projector using a camera. They use structured light and a planar checkerboard pattern, which is unsuitable for laser projectors, as they cannot project the required light pattern. A more suitable approach is proposed in [5] using a checkerboard mounted on a planar surface with the projector projecting a circle grid onto the same surface. The image taken by the camera of both the physical checkerboard pattern and the projected circle grid on the same plane can be used to estimate the required optical parameters of the projector. Although the laser projector cannot project a circle grid, the grid can be easily replaced by a point grid, making the method suitable for laser projectors.

3 Camera-Laser Sensor System

A laser projection-based AR setup requires calibration of the utilized components to accurately detect and consequently project information in the correct place. More specifically, we require an understanding between the two-dimensional images projected by the projector and the three-dimensional environment on which they are projected. To establish this relationship, we incorporate a camera in our setup. We employ camera-laser stereo calibration to calibrate both the laser projector and the camera, and an oblique projection correction to make our setup applicable on skewed surfaces.

3.1 Camera, Laser and Camera-Laser Calibration

According to Bimber and Raskar [3], a projector can be seen as an inverse camera. Instead of capturing a 2D projection of the 3D world like a camera, the projector projects a 2D image into the 3D world. This equivalence is convenient as it allows us to model both the projector and the camera in the same way by applying the pinhole model. Hence, we use the mathematical model of the *pinhole camera*. This well-known concept is widely used in the literature [13] and describes the geometric proportions inside cameras.

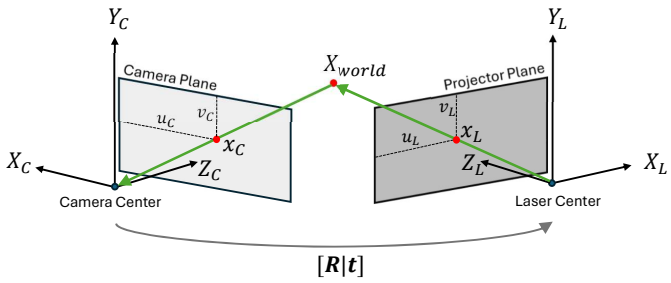

Figure 2: Laser-camera stereo setup with each device modeled as a pinhole camera. Note that the laser beam emerges from the laser center.

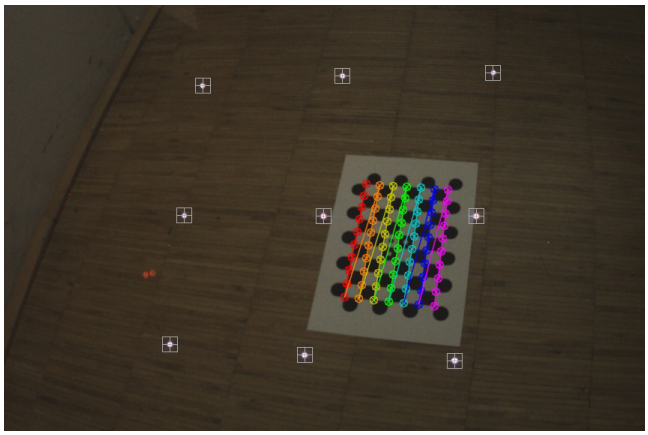

Figure 3: Visualization of the calibration grid used for the projector calibration with the detected chessboard corners and grid points. Note that for the ground plane estimation, only the projected grid points, *i.e.,* the white points, are required.

3.1.1 Camera Calibration

Given a point $X \in \mathbb{R}^3$ in the three-dimensional camera coordinate system, we can describe its position on the image plane by drawing a line between X and the center of the camera $C \in \mathbb{R}^3$. The point at which this line intersects the image plane is the position at which we will find the 2D representation $x \in \mathbb{R}^2$ of X in the image, as shown as the camera model in Fig. 2. The similarity to a laser projector is apparent, as the above-mentioned line from the camera center C to an arbitrary point X is analogous to a laser beam pointing to that very point. The mathematical formulation of the pinhole camera model and therefore the relation between x and X can be stated as

$$\mu\, x = \mathbf{P}\, X \qquad \text{with } \mathbf{P} = \mathbf{K}\,[\mathbf{R} \mid \mathbf{t}], \tag{1}$$

with a scale factor μ, the projection matrix $\mathbf{P} \in \mathbb{R}^{3\times4}$, the intrinsic parameters $\mathbf{K} \in \mathbb{R}^{3\times3}$, and the extrinsic parameters containing the rotation matrix $\mathbf{R} \in \mathbb{R}^{3\times3}$ and translation vector $\mathbf{t} \in \mathbb{R}^{3\times1}$. Finally, lens imperfections that lead to distortions in the acquired image must be considered. Unlike a camera, a laser projector does not exhibit lens distortions because there is no lens involved in projecting the image.

To calibrate a sensor with the pinhole model, correspondences between real-world positions and their corresponding image position are necessary. For cameras, this is done with one of the standard calibration toolboxes, *e.g., OpenCV* [4]. Essentially, images containing a pattern of known size are acquired and the known calibration pattern is detected. This yields 2D-3D correspondences which are utilized to solve Equation (1) and if needed, to estimate the polynomial coefficients considering the distortion coefficients [13].

3.1.2 Laser Calibration

The idea of using a calibration pattern with known geometry and detecting it in the image to obtain 2D-3D correspondences cannot be applied to projectors as they do not take images but project them. Moreover, if we project a point, we know its 2D position on the projector image plane, but we lack the knowledge of where the point ends up in the 3D world.

To obtain the relationship between the 3D world and the projected points, *i.e.,* the intersection between the laser beam and an object, we use the calibrated camera in conjunction with a printed chessboard pattern similar to [5]. More specifically, we project a grid of points on a planar surface next to a calibration pattern, as seen in Fig. 3. To simplify the conversion, we define a new world coordinate system, *i.e.,* the *board coordinate system*, which lies at $Z = 0$ and is defined by the planar calibration pattern. First, we find a homography $\mathbf{H}_{IP} \in \mathbb{R}^{3\times3}$ that transforms between the camera image plane and the projection plane, *i.e.,* that board coordinate system. $\mathbf{H}_{IP}$ can be estimated using the 2D image coordinates of the checkerboard corners and their respective 2D board coordinates. Next, using $\mathbf{H}_{IP}$, we transform the 2D image coordinates of the projected grid points into 2D board coordinates as

$$p_{board} = \mathbf{H}_{IP}\; p_{image}. \tag{2}$$

Finally, we can get 3D board coordinates for the grid points by appending a Z-coordinate set to zero to the 2D board coordinates we calculated. This is valid because the 2D board coordinate system is just a 2D coordinate system defined on the Z-plane of the 3D board coordinate system with the same origin and XY-base vectors as described above. Using the position of the grid points in the projected image and their respective 3D board coordinates as 2D-3D correspondences, we can calibrate the laser projector the same way as the camera.

3.1.3 Stereo Calibration

The camera and projector are mounted in the same enclosure, forming a cohesive camera-projector setup. In addition to the intrinsic camera and projector parameters, we require the relative position and orientation between both devices. In the classic stereo calibration workflow [13], features are matched between adjacent views to estimate the extrinsics between them. However, as we already know the coordinates of the projected grid in the camera and the projector image, we simply utilize these correspondences to obtain the stereo calibration. The stereo model of the camera projector is visualized in Fig. 2.

3.2 Oblique Projection

When projecting on skewed surfaces, the optical axis of the projector is not aligned with the projection screen. Bimber and Raskar [3] call this kind of projection *oblique projection* and further note that the projected images exhibit perspective distortion. To compensate for such distortions, we should estimate the skewed ground plane and alter our projection image accordingly. For this, an arbitrary point grid can be projected and detected with the camera image obtained. Then we apply triangulation between the known positions of the points in the projection plane, the known position of the grid in the camera image, and the unknown points on the ground plane. This triangulation is possible, as we obtained the camera parameters of both the camera and the laser in our calibration routine.

Using the detected plane and the triangulated 3D grid points, a 2D coordinate system can be estimated in the ground plane and a homography $\mathbf{H}_{GP}$ between the ground plane and the projector can be estimated. Finally, this homography is applied to the points of a graphic defined in the 2D ground plane coordinate system, giving us the points of the graphic in the projector image. By applying the homography, the graphic that appears on the skewed ground plane will be the graphic we initially defined in the 2D ground plane coordinate system. Thus, homography $\mathbf{H}_{GP}$ can be used to draw graphics in the ground plane without distortion.

The homography estimation requires point correspondences between the 2D projector image coordinate system and the 2D ground-plane coordinate system. For these correspondences, the projected grid points are reused, as they allow us to calculate the 2D coordinates of the grid points on the ground plane. Note that the origin of the 2D ground-plane coordinate system can be defined arbitrarily since only the relative positions of the points w.r.t. each other are relevant for the homography.

An example of an oblique projection of a *STOP* sign can be seen in Fig. 4. In a usual fronto-parallel projection on a wall, the sign appears undistored. When the prototype is tilted so that the primitive is projected onto the ground, a significant distortion becomes visible.

Figure 4: (Left) A projected *STOP* sign appears distorted from the laser's viewpoint after tilting the projector roughly 45°. (Right) The same sign appears undistorted after applying our oblique projection workflow.

After we apply the workflow described above, the stop sign is again undistorted from the prototype's viewpoint.

4 Prototype

Our evaluation prototype consists of a laser projector, a camera, and a single-board computer (SBC) acting as a local controller. These devices, together with a switch and a power distributor, were mounted inside an enclosure to create an independent unit, as shown in Fig. 5. A list of components is given in Table 1. This unit can communicate with an external computer via a single Ethernet cable. Power for the setup is also supplied by a single cable and distributed to the individual hardware components. Thus, only two cables are exposed, allowing easy testing in the field. The hardware setup requires approximately 70W of power: 40W for the laser projector, 15W for the single-board computer, and 12W for the switch. The camera module requires less than 500mW and is powered by the single-board computer's USB port.

4.1 Software System Architecture

To control the hardware unit, we developed the *AR client application*, *i.e.,* a software implementation that controls the hardware and implements most of the functionality described in the following sections. In addition to this application, we allow for a second component, which is an external computer outside the hardware unit connected via the exposed Ethernet cable, which we call the *external host*. The two components communicate over a TCP/IP network using the message queuing telemetry transport (MQTT) protocol [15].

In this system, the main task of the external host is to define *what* should be projected, while the AR client app on the NanoPi SBC is concerned with *how* to project it. Furthermore, the MQTT-based interface allows for convenient control of all components within the hardware unit via the external host.

4.2 Laser Graphics Pipeline

Unlike a computer screen, a laser projector does not display raster graphics, but is more similar to a vector display. Graphics are drawn by a single beam on a continuous path while modulating laser modules to create colors or blank segments [26]. This path representing the entire image is sent to the projector as a set of points, each point having a position and a color. Hence, we propose a pipeline that converts the unsorted list of line segments into a set of points for the laser projector. This process is illustrated in Fig. 6. In addition, we describe the optimizations necessary to ensure an accurate projection and prevent damage to the projector optical system. The optimizations pose the last step of our laser graphics pipeline.

Laser Projector	*Laserworld DS-1000RGB MK3*
Single Board Computer	*NanoPi NEO4 1GB*
Network Switch	*Netgear GS108*
Camera	*Arducam AR0134*

Table 1: Main hardware components integrated into our prototype.

4.2.1 Clipping

Since the projector has a bounded FOV and the line segments are defined in the unbounded projector image plane, we clip the line segments as a first step in our pipeline. More specifically, the X- and Y-coordinates are sent to the projector as 16-bit unsigned integers, where the number range spans the entire width/height. Hence, the points at position $(0,0)$ and the point at position $(2^{16}-1, 2^{16}-1)$ are at diagonally opposite corners. Thus, if a point is outside of the image, its coordinates overflow and the point will be displayed at some wrong position in the image.

All line segments outside the projector image must be removed to avoid that issue. Additionally, line segments that are partially outside of the image have to be shortened so that both endpoints lie within the visible image. For this, we apply the *Cohen-Sutherland* line clipping algorithm [9] to all line segments. Note that by performing clipping first, we avoid problems that might occur when clipping is performed after paths are planned. Furthermore, for all further steps, we can assume that the points with which we are working lie within the projector image.

4.2.2 Clustering Line Segments to Paths

Line segments are neither arbitrary nor independent. If we, for example, draw a Bézier curve, a set of connected line segments will be created that represent a discretization of the curve. Ideally, we want to draw all line segments of this curve in one continuous motion without jumping around between the curve and other objects, as that would cause visual artifacts such as discontinuities in the curve.

We achieve that by clustering connected line segments into subpaths and only allowing jumps between those subpaths and not between individual line segments. The rationale for creating subpaths instead of remembering which line segments belonged to which primitive and drawing the primitives in one continuous path is that a primitive that once was a single path might now be two or more paths if parts of the primitive were clipped away. Moreover, we might have constructed shapes out of multiple primitives, like a polygon made up of several lines. By clustering the line segments, such shapes will be contained in the same path and thus be drawn continuously.

4.2.3 Building a Continuous Path

Finally, since the laser projector projects an image by moving a laser beam in one continuous motion, we have to construct a single superpath that contains all subpaths. We obtain such a path by connecting the subpaths with *blank lines* which are invisible lines drawn with the laser modules turned off. Because it takes time to move the mirrors that deflect the laser beam from one position to another, the longer the path representing the image, the longer it takes to project that image. If the images take a long time to project, the frame rate drops and flicker occurs. Therefore, to reduce flickering, we want to connect the subpaths while minimizing the length of the blank lines and, thus, the length of the superpath that the laser projector has to project.

We distinguish between two kinds of paths: open paths and closed paths. An open path starts at some position and ends at another, whereas a closed path starts and ends at the same position. The kind of path limits the number of positions at which we can start drawing the path. An open path can only be drawn continuously, starting at one of its endpoints. Therefore, for an open path, we only have

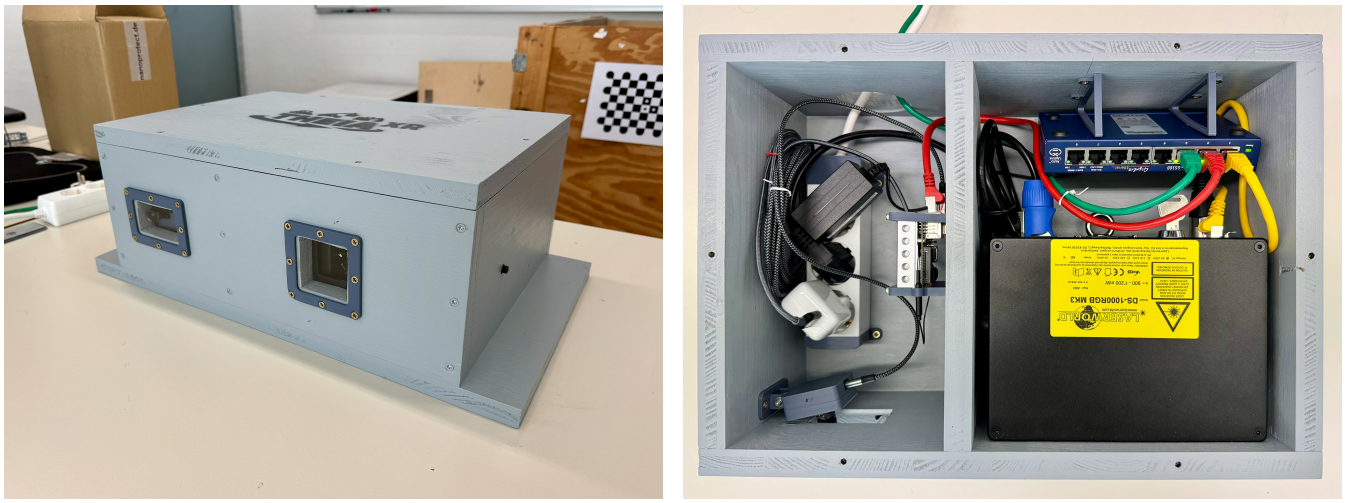

Figure 5: (Left) Image of the proposed prototype with the camera aperture on the left sight and the aperture for the laser projector on the right side. The baseline between both devices is 23 cm. (Right) Open prototype showing the internal components.

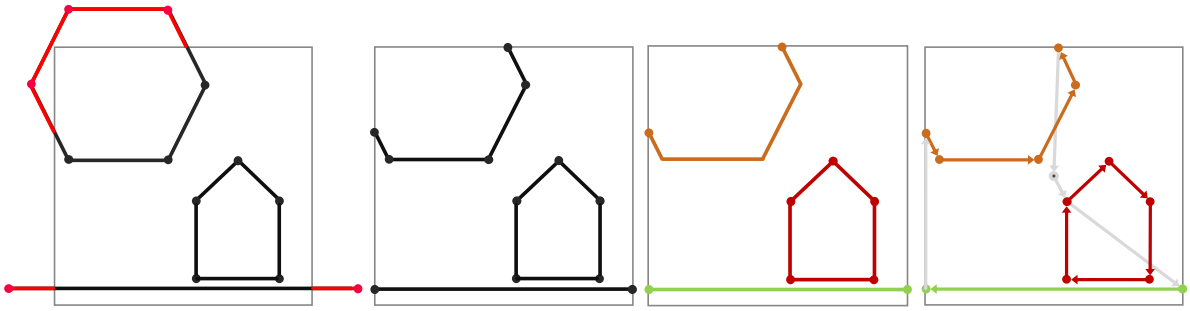

Figure 6: Examples of the separate steps in the proposed laser graphics pipeline. From left to right, the figures depict initial line segments, clipped line segments, line segments clustered into paths, and the final continuous path.

to consider the two endpoints. On the other hand, a closed path can be drawn starting at either of its vertices, which means that a closed path with n line segments can be drawn starting at n different positions.

Finding an ideal superpath through all subpaths is a difficult problem related to the *Generalized Traveling Salesman Problem* (GTSP), which is known to be NP-hard [18]. Considering that for the application at hand, we require a real-time projection of frames solving a GTSP instance optimally, or even using more involved heuristics would be too slow. For that reason, we implemented a fast but coarse approximation using a nearest-neighbor heuristic.

4.2.4 Optimizations

In theory, the list of points is sufficient to draw the image by sequentially moving the laser beam through their positions while setting the power output of the laser modules to the color of the point drawn last. However, in reality, some physical limitations and inaccuracies have to be taken into account to avoid damage to the optical systems and to ensure an accurate projection of the image. Therefore, as a final step in the pipeline, we perform multiple optimizations on the list of points. Those optimizations are inspired by the optimization and post-processing steps described in the *Showcontroller* software manual [1], a laser show software developed and distributed by the manufacturer of the laser projector that we use for this project.

Overall, the proposed optimization steps slow down the laser beam but increase the accuracy of the image drawn. It is crucial to tune the parameters of all optimization steps so that we introduce the least amount of speed reduction while still achieving high projection quality. Also, each optimization is dependent on the utilized hardware and may or may not be necessary when a different laser projector is used.

Maximum Step Size The *step size* refers to the distance between two consecutive points. A laser projector projects points at a certain scan speed defined in points per second. Therefore, a single point has to be projected within a period equal to one divided by the scan speed. If the step size between two points is large, the optical scanning system has to move its mirrors at a high speed, which leads to increased stress on the mechanical system. Additionally, the images produced with large step sizes would suffer from severe optical defects. Thus, to protect the optical scanning system and to produce useful images, we reduce the step size by inserting additional points between large jumps. As a small maximum step size would cause flickering, the chosen maximum step size should be defined as small as necessary to avoid damage and optical defects and as big as possible to keep the number of additional points low.

Color Shifting Whenever the laser beam arrives at a point with a different color than the point before, the laser modules are adjusted to produce the new color. This is done so that the line between the current and the next point is projected with the correct color. In reality, the synchronization between the optical scanning system moving the beam and the laser modules controlling the color is not perfect. As a result, the color of the beam might change slightly before or after it reaches the position at which the color change is supposed to occur. The resulting artifact is depicted in the upper left image of Fig. 7. One possible solution to address this problem is to modify the colors. Depending on whether the color change happens

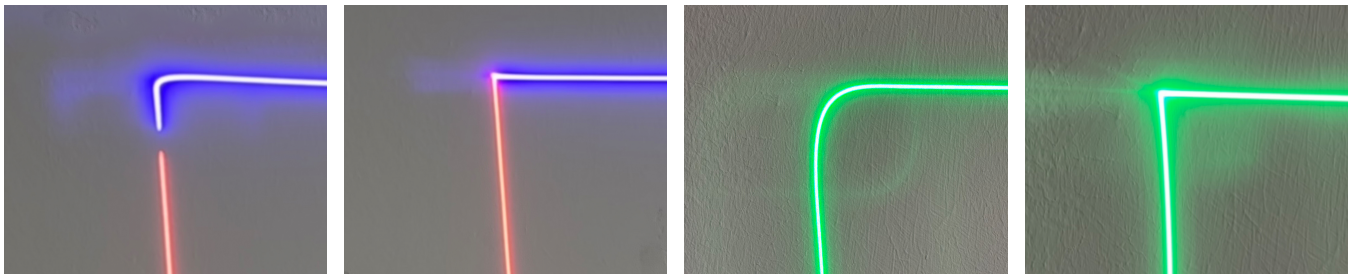

(a) (b) (c) (d)

Figure 7: Images showing the effect of the optimization measures. (Left) Examples of the effect of our optimizations w.r.t. on the change in color (a) before and (b) after optimization. (Right) The corner in (c) is rounded, while it is drawn sharper in (d) due to corner point repetition.

too early or too late, we move the color of each point to the point before or after. We can also shift the colors over multiple points, *i.e.,* shift by $\pm m$ points so that the new color of the i^{th} point is the color initially assigned to point $i \pm m$.

Extra Points around Color Changes Color shifting alone can not fix the synchronization error sufficiently due to the attainable time offset, which is always a multiple of the time it takes to project a single point. Moreover, the error is dependent on the distance between the points, or whether the color change occurs on a line or at a position where the beam has to change directions. Therefore, we add another optimization step that adds extra points before and after each color change at the same position as the color change. By adding points *before* the color change, the beam stays at the position of the color change a little longer before switching to the new color. This gives the optical scanning system time to catch up and can thus be used if the color changes occur too early. Similarly, adding points *after* the color change means that the beam in the new color pauses for a moment before continuing on its path. This, in turn, gives the laser modules some time to catch up and can be used to compensate for color changes that occur too late. Together with color shifting, the extra points around color changes successfully fix the synchronization issues, as can be seen in the top right image of Fig. 7.

Corner Point Repetition When the projector is operating at speed, artifacts are observed in corners (see the image at the bottom left of Fig. 7). Hence, instead of 90-degree angles, round corners appear. This problem is more pronounced at higher scan speeds and scan angles. The maximum scan angle is essentially the FOV of the projector, defining which part of the projector image we use. To counteract the resulting artifacts, we apply corner point repetition: Every corner point, that is, a point between two consecutive lines at an angle, is repeated multiple times to give the optical scanning unit more time to deflect the beam to the corner point. The number of repetitions again has to be tuned for the projector and the application at hand. The result of the final corner after our optimizations is shown in the bottom right image of Fig. 7.

5 Evaluation and Use-Cases

Our setup is suitable for applications with different levels of knowledge about the environment, as our software architecture provides an interface between virtual environments and the hardware unit. We consider two different options for the presentation of information, namely the presentation of information *registered to the vehicle* and information *registered to the environment*. The former of these options can be considered as a large projection screen that follows the vehicle while operating. However, heavy machinery often features highly accurate location tracking sensors, such as differential GPS, for example. In certain cases, even a full 3D model of the environment is available, which enables us to place the machinery, respectively, the laser projector, into an environment with existing structures to be visualized. Therefore, we evaluate our approach in a reconstructed 3D environment, in which we evaluate how accurately we can project primitives at a distance of up to 25m. Furthermore, we propose two different types of application, both suitable for various types of heavy machinery. Finally, we discuss the known limitations of our prototype.

5.1 Projector Accuracy

Here, we first intend to answer the question: *Given a target position in the projector image, how accurately can our prototype highlight this position?* We design our evaluation based on the experiments performed by Hansen *et al*. [12]. Thus, we project primitives on known target points with varying distances and measure the deviation in the vertical and horizontal directions. The 3D reconstruction, as well as a schematic outline of our experimental setup within that reconstruction, can be seen in Fig. 8.

5.1.1 Setup

As a testing environment, we chose a corridor with a length of 30m and a width of 3.5m. We use a measuring tape as well as the digital laser measurement *BOSCH PLR 30* (with accuracy $\pm 2.0mm$) to obtain our distance measurements. We use a complete 3D reconstruction of the testing environment in which we register our prototype. To eliminate possible errors related to localization in our evaluation environment, we first project lines in the middle of our projection image through the AR client application, *i.e.,* without using the 3D reconstruction. We then align the prototype such that all the projected lines are equidistant from the floor. This also ensures that our evaluation environment is properly aligned with our prototype. Furthermore, we made sure that the point projected in the center of the projection image, *i.e.,* at projector coordinates $(\frac{2^{16}}{2}, \frac{2^{16}}{2})$, is projected in the same height from the ground as our laser projector, *i.e.,* 0.993m. Finally, we placed the prototype in the 3D reconstruction in the same spot as in the physical corridor. To measure the accuracy of the laser projector utilized, we then proceed to project octagons with a radius of 1m on the ground at varying distances. Finally, we measure the distances from the center point of the octagon, *i.e.,* the target of our projection, and the vertices parallel and perpendicular to the projector's optical axes.

5.1.2 Results

As the laser beam is essentially a cone, an intersection with an inclined plane reveals an elliptic cross section of this cone. The distortion and size of this cone increase with the shallowness of the projection angle and with the projection distance, respectively. To measure the distance, we take the vertices of the respective elliptic cross sections, *i.e.,* the maximum and minimum illuminated distances in each direction. In Fig. 9, the elliptic cross section of the projected primitive is clearly visible. However, the image taken from a viewpoint near the projector reveals a sharp projection. Therefore,

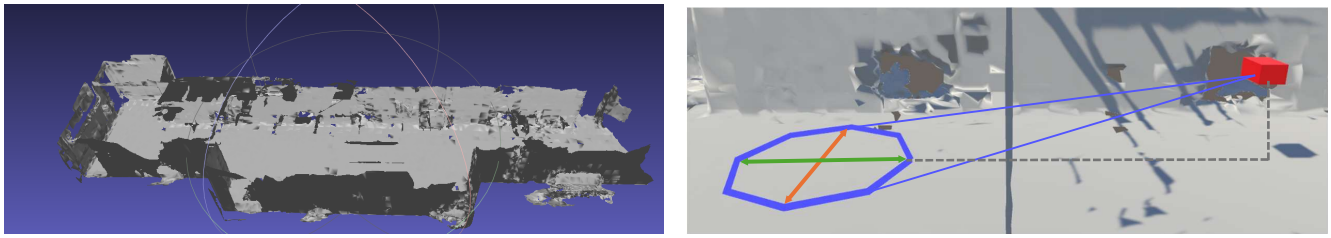

Figure 8: (Left) 3D reconstruction of our evaluation environment. (Right) The projected primitive, *i.e.,* the blue octagon is projected via line renderer in *Unity*. The red box indicates the position of our prototype in the 3D reconstruction. The orange and green arrows correspond to the measurements taken to evaluate the projection accuracy.

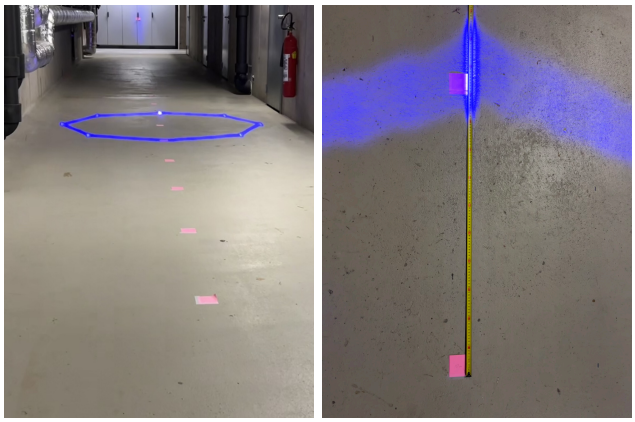

Figure 9: (Left) Cropped view from a viewpoint with a similar height as our evaluation setup. (Right) A tape measure at the upper edge of the projected primitive. The projection distance in the depicted test is 10m. As one can see, the octagon is sharply visible from the projector height even though the elliptic cone intersection is substantial.

the distortion is only substantial from viewpoints distinct from the prototype's projection angle.

The results of this evaluation can be seen in Table 2 and in Fig. 10. Note that the projection accuracy up to an evaluated length of about 25m is sufficient to project schematics with reasonable accuracy. The deviations on the vertical projection axis reveal inaccuracies in proximity to the projector. This is likely due to the prototype's location in our environment. Since the prototype is mounted perpendicular to the ground plane, the projector has to maximize its vertical operating angle to project these points. With a tilted mounting angle, the projection would not suffer from such inaccuracies. However, we designed this evaluation in a way to provide a worst-case estimate of the deviations.

5.2 Use-Cases

Our workflow allows for two applications, namely the projection on the ground and the projection into aerosols, *e.g.,* fog. Here, we elaborate on those use cases and discuss them with regard to the necessary amount of environmental information.

5.2.1 Projection on the Ground

The proposed setup can be used to project information on the ground ahead of any heavy machinery, as illustrated in Fig. 1 and Fig. 4. For example, a virtual perimeter can be drawn around potential hazards, such as rocks, ledges, or artificial structures, to warn the operator. Similarly, information about the vehicle can be displayed, such as the predicted path of the machine based on the current steering angle, to assist the operator in maneuvering. Furthermore, the laser projector can directly mark lanes on the ground, which not only simplifies

Distance [m]	Y-Axis		X-Axis	
	Size [m]	Δ [m]	Size [m]	Δ [m]
1	0.015	0.313	0.023	0.001
2	0.033	0.279	0.024	0.014
3	0.05	0.195	0.032	0.007
5	0.103	0.106	0.035	0.043
7.5	0.163	0.031	0.05	0.055
10	0.29	0.03	0.061	0.064
12.5	0.36	0.045	0.063	0.062
15	0.575	0.043	0.06	0.06
20	0.875	0.068	0.05	0.055
25	1.55	0.075	0.06	0.06

Table 2: Results of our accuracy evaluation. The size corresponds to the absolute distance between the minimum and maximum measured values. The Δ-values yield the deviations from the target points, *i.e.,* 1m in the horizontal (Y) and vertical (X) direction from the center of the octagon.

navigation by offering a visual guide, but also eliminates the need to consult a map on a separate display.

By exploiting the visibility of projection-based AR beyond the operator, the system can display warnings to people or colleagues to reduce the risk of accidents. For example, cameras or additional sensors could detect people around the vehicle to project customized warnings in front of them.

5.2.2 Projection into Aerosols

Heavy machines are usually operated in any weather condition. In these situations, projections on the ground are less useful as only a very limited part of the ground close to the vehicle is visible. Therefore, we can project directly into the aerosols, *e.g.,* fog or snow, taking advantage of the fact that laser beams become visible on impact with them, an effect known from clubs and stage shows.

For example, in poor visibility conditions, machines may be at risk of colliding with structures. Given a 3D reconstruction of the environment and precise location of the vehicle, we can trace the outlines of those structures with our prototype, creating rays between the projector and the structures. Those rays are visible in the fog surrounding the vehicle and can give the operator an idea of where the structures are located even when they are beyond the visible range. The concept could be extended by using different colors depending on the distance, thus providing additional information about the object's location. As a final resort, if a vehicle gets too close to an obstacle, the projector can be utilized to create a virtual wall by projecting a line in front of the snow groomer. This line would appear to the operator as a plane tilted in front of the vehicle.

To demonstrate this use-case by simulating a 3D reconstruction of a real mountain environment together with a snow groomer. Within that simulated 3D environment, we define a set of contours that the laser projector should trace, assuming that the projector is mounted on the snow groomer facing forward. We use a wall as a projection

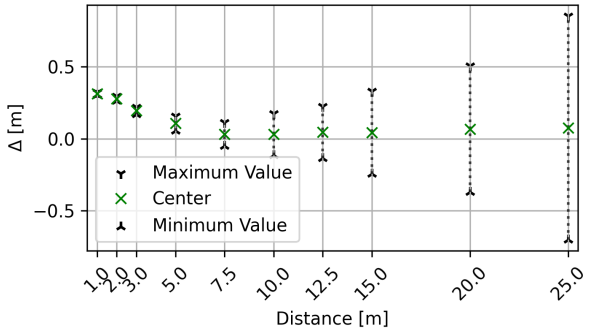

(a) Absolute vertical deviation in our experimental setup.

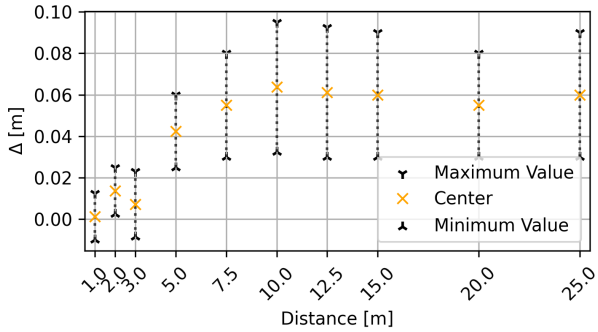

(b) Absolute horizontal deviation in our experimental setup.

Figure 10: Visual representation of the evaluation results. The size of the laser on the ground is indicated with minimum and maximum values. The deviation Δ between the measured center point and the projected distance (1m) of the octagonal primitive is measured in vertical (a) and horizontal (b) directions.

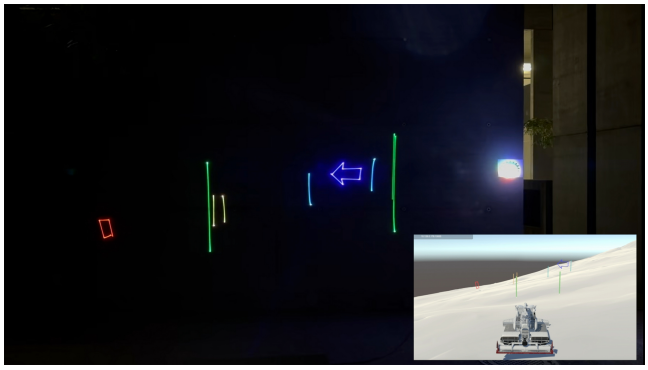

Figure 11: Real-world test of projecting 3D contours using a simulated snow groomer and a wall as a projection surface.

surface and mount the projector facing the wall, imitating the fog. Fig. 11 provides an image of this demonstration, with a screenshot of the simulated environment in the corner.

6 Discussion

We acknowledge that our prototype has certain limitations that require further investigation. In general, most laser projector systems are targeted at customers in the entertainment industry. Inherently, the projector might provide insufficient accuracy for some use cases. However, this could be mitigated by switching to other hardware or by evaluating different types of laser projectors on the market.

Our proposed pipeline proved fast enough to sustain a reasonable number of frames per second, and the paths produced are enough to create recognizable and sharp projections. However, some visual artifacts remained, which warranted additional efforts to further optimize the pipeline. In particular, the motion of objects in between frames can cause a sudden change in the path returned by the nearest neighbor search *e.g.,* when primitives move closer or farther away from each other. Since minor visual artifacts remain even after the optimizations, those jumps also lead to sudden changes in those artifacts, making the animations appear choppy and uneven. To fix this issue, we have to consider the previous image in addition to the current one during pathfinding and avoid changes in the new path when possible. In addition, returned paths can be improved by using more elaborate pathfinding methods to minimize their length.

Detecting projected points as detailed in Sect. 3.1 only works reliably in a dark environment. This is because we used a long exposure time to avoid the problem of missing points in the camera image described above. Thus, if the environment is too bright, the images are overexposed, and the detection becomes unstable.

Finally, in this project, we consider the surface of the ground as a plane to simplify the modeling of distortions. This assumption will only work in some cases. If the ground is uneven or has a curvature, distortions that our simplified model cannot remove will occur. A more accurate approach would be to create a ground mesh instead of a ground plane and use this mesh to create undistorted projections. When detecting the ground plane, we already generate a mesh that can be used for that purpose. We might also use this mesh for other applications, such as continuously building a 3D reconstruction of the environment while operating.

7 Conclusion

This work explores the implementation and use of laser projection-based AR as a concept to work in the application field of heavy machinery. We present a compact and weather-resistant unit suitable for real-world tests on off-highway machinery that contains a laser projector, a camera, and a single-board computer. Moreover, we outline a flexible software system for the hardware unit, enabling applications running on an external computer to use our setup through a convenient MQTT interface. Additionally, we detail a calibration process to calibrate the camera projector setup based on existing calibration methods. In addition, we present a method to calculate the geometric properties of the ground surface in front of the projector. This information is then utilized to generate projections that are free from distortion and have accurate dimensions on the identified surface. Finally, we conduct experiments to showcase the accuracy of our setup.

Note

Testing the system with our partners in a real environment on heavy machinery with an existing 3D model of the environment is already scheduled for the end of January 2024. Therefore, we are looking forward to having video materials and images of the system in action by the beginning of February 2024.

Acknowledgments

Funded by the European Union under Grant Agreement No. 101092861. Views and opinions expressed are, however, those of the author(s) only and do not necessarily reflect those of the European Union or the European Commission. Neither the European Union nor the granting authority can be held responsible for them. We express our gratitude to Emma Stettner for illustrating Fig. 1.

REFERENCES

[1] L. AG. User Manual Showcontroller Laser and Multimedia Software. https://www.laserworld.com/en/download-file-1699-Showcontroller_User_Manual___EN.html, 2019. Online; accessed November 9, 2023.

[2] S. Aromaa, V. Goriachev, and T. Kymäläinen. Virtual Prototyping in the Design of See-Through Features in Mobile Machinery. *Virtual Reality*, 24:23–37, 2020.

[3] O. Bimber and R. Raskar. *Spatial Augmented Reality: Merging Real and Virtual Worlds*. CRC press, 2005.

[4] G. Bradski. The OpenCV Library. *Dr. Dobb's Journal of Software Tools*, 2000.

[5] A. Cassinelli. Easy Camera-Projector Calibration. https://alvarocassinelli.com/easy-camera-projector-calibration/, 2012. Online; accessed November 30, 2023.

[6] Y. Chen, X. Wang, and H. Xu. Human Factors/Ergonomics Evaluation for Virtual Reality Headsets: A Review. *Transactions on Pervasive Computing and Interaction*, 3(2):99–111, 2021.

[7] H.-L. Chi, S. Kang, S. Hsieh, and X. Wang. Optimization and Evaluation of Automatic Rigging Path Guidance for Tele-Operated Construction Crane. In *Proceedings of the International Symposium on Automation and Robotics in Construction*, vol. 31, 2014.

[8] Y. Fang and Y. K. Cho. Effectiveness Analysis From a Cognitive Perspective for a Real-Time Safety Assistance System for Mobile Crane Lifting Operations. *Journal of Construction Engineering and Management*, 143(4), 2017.

[9] J. D. Foley. *Computer Graphics: Principles and Practice*, vol. 12110. Addison-Wesley Professional, 1996.

[10] N. D. Glossop and Z. Wang. Laser Projection Augmented Reality System for Computer-Assisted Surgery. In *Proceedings of the Medical Image Computing and Computer-Assisted Intervention*, 2003.

[11] E. Halbach and A. Halme. Job Planning and Supervisory Control for Automated Earthmoving Using 3D Graphical Tools. *Automation in Construction*, 32:145–160, 2013.

[12] L. H. Hansen, P. Fleck, M. Stranner, D. Schmalstieg, and C. Arth. Augmented Reality for Subsurface Utility Engineering, Revisited. *Transactions on Visualization and Computer Graphics*, 27(11):4119–4128, 2021.

[13] R. Hartley and A. Zisserman. *Multiple View Geometry in Computer Vision*. Cambridge University Press, 2003.

[14] L. J. Hettinger and G. E. Riccio. Visually Induced Motion Sickness in Virtual Environments. *Presence: Teleoperators & Virtual Environments*, 1(3):306–310, 1992.

[15] G. Hillar. *MQTT Essentials - A Lightweight IoT Protocol*. Packt Publishing, 2017.

[16] Y. Kaizu and J. Choi. Development of a Tractor Navigation System Using Augmented Reality. *Engineering in Agriculture, Environment and Food*, 5(3):96–101, 2012.

[17] D. Moreno and G. Taubin. Simple, Accurate, and Robust Projector-Camera Calibration. In *Proceedings of the International Conference on 3D Imaging, Modeling, Processing, Visualization & Transmission*, 2012.

[18] C. E. Noon. *The Generalized Traveling Salesman Problem*. University of Michigan, 1988.

[19] M. E. Rakauskas, N. J. Ward, A. R. Gorjestani, C. R. Shankwitz, and M. Donath. Evaluation of a DGPS Driver Assistive System for Snowplows and Emergency Vehicles. In *Proceedings of the International Conference of Traffic and Transport Psychology*, 2005.

[20] R. Raskar, J. Van Baar, P. Beardsley, T. Willwacher, S. Rao, and C. Forlines. iLamps: Geometrically Aware and Self-Configuring Projectors. In *Proceedings of the International Conference on Computer Graphics and Interactive Techniques*, 2006.

[21] R. Raskar, G. Welch, and H. Fuchs. Spatially Augmented Reality. *Augmented Reality: Placing Artificial Objects in Real Scenes*, pp. 64–71, 1999.

[22] R. Raskar, G. Welch, K.-L. Low, and D. Bandyopadhyay. Shader Lamps: Animating Real Objects With Image-Based Illumination. In *Proceedings of the Eurographics Workshop*, pp. 89–102, 2001.

[23] B. Sarupuri, G. A. Lee, and M. Billinghurst. Using Augmented Reality to Assist Forklift Operation. In *Proceedings of the Australian Conference on Computer-Human Interaction*, pp. 16–24, 2016.

[24] B. Schwerdtfeger, D. Pustka, A. Hofhauser, and G. Klinker. Using Laser Projectors for Augmented Reality. In *Proceedings of the ACM Symposium on Virtual Reality Software and Technology*, 2008.

[25] T. A. Sitompul and M. Wallmyr. Using Augmented Reality to Improve Productivity and Safety for Heavy Machinery Operators: State of the Art. In *Proceedings of the Conference on Virtual-Reality Continuum and its Applications in Industry*, 2019.

[26] P. L. Systems. Laser Show Projectors Explained. https://pangolin.com/blogs/education/laser-show-projectors-explained, 2016. Online; accessed March 28, 2023.

[27] R. Tsai. A Versatile Camera Calibration Technique for High-Accuracy 3D Machine Vision Metrology Using Off-The-Shelf TV Cameras and Lenses. *IEEE Journal on Robotics and Automation*, 3(4):323–344, 1987.

[28] M. Wallmyr, D. Kade, and T. Holstein. 360 Degree Mixed Reality Environment to Evaluate Interaction Design for Industrial Vehicles Including Head-up and Head-Down Displays. In *Proceedings of the International Conference on Virtual, Augmented and Mixed Reality*, pp. 377–391, 2018.

[29] M. F. Zaeh and W. Vogl. Interactive Laser-Projection for Programming Industrial Robots. In *Proceedings of the Symposium on Mixed and Augmented Reality*, 2006.

[30] Z. Zhang. A Flexible New Technique for Camera Calibration. *IEEE Transactions on Pattern Analysis and Machine Intelligence*, 22(11):1330–1334, 2000.